

Published in final edited form as:

*Neuron*. 2014 October 1; 84(1): 164–176. doi:10.1016/j.neuron.2014.08.058.

## Phasic dopamine release drives rapid activation of striatal D2-receptors

Pamela F Marcott<sup>1</sup>, Aphroditi A Mamaligas<sup>2</sup>, and Christopher P Ford<sup>1,2</sup>

<sup>1</sup>Department of Physiology and Biophysics, Case Western Reserve University School of Medicine, 10900 Euclid Ave, Cleveland, OH, 44106-4970

<sup>2</sup>Department of Neurosciences, Case Western Reserve University School of Medicine, 10900 Euclid Ave, Cleveland, OH, 44106-4970

### Summary

Striatal dopamine transmission underlies numerous goal-directed behaviors. Medium spiny neurons (MSNs) are a major target of dopamine in the striatum. However, as dopamine does not directly evoke a synaptic event in MSNs, the time course of dopamine signaling in these cells remains unclear. To examine how dopamine release activates D2-receptors on MSNs, G-protein activated inwardly rectifying potassium (GIRK2;  $K_{ir}$  3.2) channels were virally overexpressed in the striatum and the resulting outward currents were used as a sensor of D2-receptor activation. Electrical and optogenetic stimulation of dopamine terminals evoked robust D2-receptor inhibitory post-synaptic currents (IPSCs) in GIRK2-expressing MSNs that occurred in under a second. Evoked D2-IPSCs could be driven by repetitive stimulation and were not occluded by background dopamine tone. Together, the results indicate that D2-receptors on MSNs exhibit functional low affinity and suggest that striatal D2-receptors can encode both tonic and phasic dopamine signals.

### Introduction

Dopamine transmission in the striatum plays a central role in multiple motivationally relevant behaviors (Schultz, 2007a). Dysfunctions in dopamine signaling underlie a variety of motor and psychiatric diseases including Parkinson's disease, schizophrenia and drug addiction (Meisenzahl et al., 2007; Volkow et al., 2009). Dopamine neurons fire in an asynchronous tonic pacemaker firing pattern that switches to transient synchronous bursts

© 2014 Elsevier Inc. All rights reserved.

Corresponding author: Christopher Ford (cpf21@case.edu). Address for Correspondence: Department of Physiology and Biophysics, Case Western Reserve University School of Medicine, 10900 Euclid Ave, Cleveland, OH, 44106-4970.

#### Author Contributions

PFM and CPF designed the research. PFM, AAM and CPF performed the research. PFM and CPF analyzed the data, prepared the figures and wrote the manuscript.

The authors declare no competing financial interests.

**Publisher's Disclaimer:** This is a PDF file of an unedited manuscript that has been accepted for publication. As a service to our customers we are providing this early version of the manuscript. The manuscript will undergo copyediting, typesetting, and review of the resulting proof before it is published in its final citable form. Please note that during the production process errors may be discovered which could affect the content, and all legal disclaimers that apply to the journal pertain.

following the appearance of unexpected rewards or cues predicting those rewards (Bromberg-Martin and Hikosaka, 2009; Grace and Bunney, 1984a, b; Phillips et al., 2003; Schultz, 2007a; Tobler et al., 2005).

Dopamine transients of varying duration have been identified using techniques that measure the concentration of extracellular dopamine in brain slices and awake behaving animals (Chergui et al., 1994; Garris et al., 1994; Howe et al., 2013; Phillips et al., 2003; Schultz, 2007b). Phasic dopamine transients that result from synchronous burst firing are primarily thought to activate low affinity striatal D1-receptors while background tonic dopamine levels arising from pacemaker firing maintain steady-state activation of high-affinity D2-receptors (Cragg and Rice, 2004; Grace and Bunney, 1984a; Grace et al., 2007; Keefe et al., 1993; Richfield et al., 1989; Surmeier et al., 2011). The tonic stimulation of striatal D2-receptors by basal dopamine levels is proposed to enable several cognitive and motor functions (Baik et al., 1995; Berke and Hyman, 2000; Schultz, 2007b). As aberrant changes in tonic dopamine signaling underlie numerous psychiatric diseases, blocking D2-receptors is currently the central strategy of antipsychotic therapies (Howes and Kapur, 2009; Seeman et al., 2005).

Despite the importance of D2-receptors in striatal function, the time course over which dopamine transients activate these receptors on medium spiny neurons (MSNs) has not been characterized. MSNs are the principal output cell of the striatum (Gerfen and Surmeier, 2011). In MSNs, the activation of D2-receptors does not induce a direct change in post-synaptic membrane potential but instead modulates the activity of multiple conductances through second messenger-mediated processes (Gerfen and Surmeier, 2011; Kreitzer, 2009; Nicola and Malenka, 1998; Surmeier, 2006; Tepper, 2006; Tritsch and Sabatini, 2012). The slow kinetics of these intracellular signaling cascades have limited the temporal resolution over which D2-receptor signaling can be assessed. It therefore remains unclear to what extent phasic dopamine transients are encoded by these receptors.

In the present study, an adeno-associated virus (AAV) was used to drive the expression of G-protein-coupled inwardly rectifying potassium channels (GIRK2; Kir3.2) in MSNs to provide a readout of dopamine D2-receptor mediated transmission with improved temporal resolution. Multiple  $G_{i/o}$ -coupled receptors couple to GIRK channels in other regions to evoke metabotropic IPSCs (Luscher and Slesinger, 2010). Here we found that following the overexpression of GIRK channels, efficient coupling to D2-receptors provided a new rapid sensor for measuring dopamine D2-receptor activation in MSNs.

## Results

### GIRK Channels Couple to D2-receptors in MSNs When Overexpressed

To drive the expression of GIRK2, we designed an adeno-associated virus (AAV) encoding tdTomato-GIRK2 under the control of the synapsin promoter (Figure 1A). Three weeks following injection of the vector into the striatum, fluorescence from the tdTomato reporter was widely seen in the striatum (Figure 1B). To confirm that the viral vector also drove the expression of GIRK, we counted tdTomato<sup>+</sup> cells and examined the co-localization of tdTomato with GIRK2 immunoreactivity (Figure 1B). We found that GIRK2<sup>+</sup> co-localized

with  $92 \pm 1\%$  of tdTomato<sup>+</sup> cells (782 cells, 16 sections from 3 mice), indicating that the vector efficiently increased expression of both GIRK2 and tdTomato. As previous studies have shown that the striatum expresses little endogenous GIRK2 (Karschin et al., 1996; Liao et al., 1996), no GIRK2 immunoreactivity could be observed in control striatal hemispheres from uninjected animals (Figure 1B).

To examine whether endogenous D2-receptors in MSNs would couple to overexpressed GIRK2 channels, whole cell voltage clamp recordings (holding potential of  $-60$  mV) were made from GIRK2<sup>+</sup> striatal neurons in acute slices 3–4 weeks after AAV injection. We identified MSNs by their well-defined morphological and electrophysiological characteristics, including a hyperpolarized membrane potential, low input resistance, long delay to initial spiking, and lack of a hyperpolarization-activated sag (Figure 1C) (Gerfen and Surmeier, 2011; Kita et al., 1984; Kreitzer, 2009). MSNs expressing GIRK2 displayed a similar resting membrane potential (control:  $-84 \pm 1$  mV,  $n = 24$ ; tdTomato<sup>+</sup>:  $-83 \pm 1$  mV,  $n = 19$ ,  $p = 0.5$ , Student's unpaired  $t$  test), input resistance (control:  $47 \pm 3$  M $\Omega$ ,  $n = 53$ ; tdTomato<sup>+</sup>:  $45 \pm 1$  M $\Omega$ ,  $n = 132$ ,  $p = 0.9$ , Student's unpaired  $t$  test) and rate of action potential firing following current injection (control:  $10 \pm 1$  APs,  $n = 28$ ; tdTomato<sup>+</sup>:  $11 \pm 1$  APs,  $n = 22$ ;  $p = 0.5$ , Student's unpaired  $t$  test; 300 ms, 450 pA current injection) to control neurons from the uninjected hemisphere (Figure 1D), indicating that overexpression of GIRK2 did not affect their basic membrane characteristics. MSNs comprise ~95% of striatal neurons, with approximately half being 'indirect'-pathway MSNs that express D2-dopamine receptors (Albin et al., 1989; Graybiel, 1990; Kawaguchi et al., 1995; Kreitzer, 2009; Surmeier, 2006). We found that the D2-selective agonist quinpirole, applied via a puffer pipette, evoked an outward current in 8 out of 20 GIRK2<sup>+</sup> MSNs tested ( $91 \pm 14$  pA, range: 44 to 152 pA,  $n = 8$ ), suggesting that a significant proportion of GIRK2<sup>+</sup> MSNs were indirect pathway neurons that expressed functional D2-receptor coupled channels. Bath application of quinpirole also evoked currents that were reversed by the D2-selective antagonist sulpiride (500 nM) (Figure 1E). Likewise, in the presence of the D1-receptor antagonist SCH23390 (1  $\mu$ M), the iontophoretic application of dopamine evoked large outward currents in roughly half of GIRK2<sup>+</sup> MSNs tested (12 out of 27 cells examined; average amplitude:  $131 \pm 24$  pA,  $n = 12$ ), which was blocked by sulpiride (500 nM) ( $15 \pm 3$  pA,  $n = 7$ ,  $p < 0.01$ , Student's unpaired  $t$  test) (Figure 1F). The dopamine mediated outward current was likely the result of GIRK channel activation since the current-voltage relationship revealed inward rectification and a reversal potential near the predicted potassium reversal potential ( $n = 6$ ) (Figure 1G). No outward current occurred in response to dopamine in control MSNs from uninjected animals ( $-6 \pm 1$  pA,  $n = 15$ ,  $p < 0.001$  vs. GIRK2<sup>+</sup> MSNs,  $p > 0.05$  vs. GIRK2<sup>+</sup> MSNs in sulpiride, one-way ANOVA with Tukey-Kramer post-hoc test) (Figure 1F). Thus following expression of GIRK2, functional channels were able to couple to endogenous D2-receptors in MSNs.

GIRK2 subunits can form channels either as homotetramers or heterotetramers with GIRK1 or GIRK3 subunits (Lesage et al., 1995; Luscher and Slesinger, 2010). Since GIRK1/GIRK2 (Kir3.1–3.2) heterotetramers mediate the GIRK current in many types of neurons (Karschin et al., 1996; Kobayashi et al., 1995; Liao et al., 1996), in a subset of mice we overexpressed both GIRK1 and GIRK2 subunits in MSNs by co-injection of AAV vectors coding for

GIRK1-EGFP and GIRK2-tdTomato. Dopamine mediated currents recorded from MSNs putatively expressing GIRK1/2 (EGFP<sup>+</sup>/tdTomato<sup>+</sup>) were indistinguishable from those expressing only GIRK2 (Figure S1), indicating that expressing GIRK2 subunits was sufficient to produce functional channels in these cells.

### Dopamine Release Evokes a D2-IPSC in MSNs

We next asked how the synaptic release of dopamine activates D2-receptors in MSNs. Recordings were made in the presence of NMDA, AMPA, GABA<sub>A</sub>, GABA<sub>B</sub>, muscarinic and D1 receptor antagonists. A single stimulation in the striatum evoked a robust outward inhibitory post-synaptic current (IPSC) in GIRK2<sup>+</sup> MSNs that was abolished by the D2-receptor antagonist sulpiride (500 nM) (Figure 2A). As expected, D2-IPSCs recorded in the presence of the D1-antagonist SCH23390 were observed in roughly half of all GIRK2<sup>+</sup> cells recorded (130 out of 302 cells tested). Dopamine D2-IPSCs displayed an average maximal amplitude of  $102 \pm 5$  pA ( $n = 130$ ), with the largest measuring 270 pA (Figure 2B). D2-IPSCs reversed near the predicted potassium reversal potential, which shifted as expected in the presence of increased extracellular potassium (additional 2.5 mM) (Figures S2A and S2B). No D2-IPSCs could be evoked in MSNs from uninjected hemispheres (0 out of 53 cells tested) (Figures 2A and S2C).

The rise and fall of the IPSC occurred in less than one second (Figure 2A). D2-IPSCs peaked in  $258 \pm 5$  ms, and the duration, measured at 20% of the peak, was  $541 \pm 10$  ms ( $n = 130$ ). The latency to peak of IPSCs did not correlate with amplitude ( $n = 130$ ,  $p = 0.4$ , Pearson's correlation) (Figure 2B), suggesting that the kinetics of the IPSC did not depend on the extent of GIRK2 expression. To better resolve the activation kinetics of the IPSC, currents in the presence of sulpiride were subtracted from a subset of D2-IPSCs to eliminate the stimulation artifact (Figure 2C). D2-IPSCs activated following a lag of  $55 \pm 3$  ms (time to 10%,  $n = 20$ ) and had a rise time (10 – 90%) of  $111 \pm 6$  ms ( $n = 20$ ) (Figure 2B). As previous work in the ventral tegmental area has shown that only high concentrations of dopamine (10 – 100  $\mu$ M) evoke somatodendritic D2-receptor mediated GIRK currents with similar kinetics (Courtney and Ford, 2014; Ford et al., 2009), the rapid activation of synaptic currents in MSNs suggests that a high concentration of dopamine may activate the D2-receptors mediating the IPSC.

We next directly examined the release of dopamine using fast-scan cyclic voltammetry (FSCV) to measure axonal dopamine spillover into the extracellular space. A carbon-fiber electrode was inserted into the dorsal striatum of brain slices from either uninjected control or AAV.GIRK2-injected mice and cycled (10 Hz) from  $-0.4$  V to  $+1.3$  V using a triangular waveform (400 V/s). In control striatal hemispheres, a single stimulation evoked a rise in the extracellular concentration of dopamine ( $[DA]_o$ ) (Figure 2D) (Cragg et al., 1997; Hoffman and Gerhardt, 1999; Wightman et al., 1986). There was no difference in evoked peak  $[DA]_o$  between GIRK2-expressing slices ( $0.9 \pm 0.2$   $\mu$ M,  $n = 16$ ) and uninjected controls ( $1.3 \pm 0.3$   $\mu$ M,  $n = 9$ ,  $p = 0.1$ , Mann-Whitney test) (Figure 2E), indicating that striatal expression of GIRK2 does not affect dopamine release. We confirmed the electrochemical identity of dopamine by the peak of the oxidation and reduction current in the cyclic voltammogram (Figure 2D, inset).

To determine how the time course of dopamine release related to the activation of the D2-IPSC, striatal FSCV recordings were next performed simultaneously with whole cell voltage clamp recordings from GIRK2<sup>+</sup> MSNs (Figure 2F). The carbon-fiber electrode was placed within 100  $\mu$ m of the MSN being recorded. When simultaneously measured, a single stimulation evoked an increase in [DA]<sub>o</sub> in the bulk extracellular space of  $716 \pm 120$  nM (n = 10) and a D2-IPSC of  $95 \pm 24$  pA (n = 10) (Figure 2F). The rise in [DA]<sub>o</sub> could be detected before the activation of the D2-IPSC (Figure 2F). Cyclic voltammograms were collected every 100 ms (10 Hz sampling) and aligned such that the first measurement occurred 65 ms following the electrical stimulus. A significant increase in the [DA]<sub>o</sub> could be detected even at the time when the first post-stimulus voltammogram was measured ( $234 \pm 34$  nM, n = 10,  $p < 0.01$ , Student's paired *t* test, reaching  $30 \pm 3$  % of the maximum). As currents in the presence of sulpiride were not subtracted from D2-IPSCs during these simultaneous recordings, the initial rise in the outward current at this time point was likely affected by the stimulation artifact as the IPSC was only  $5 \pm 4$  % of maximum peak ( $8 \pm 3$  pA; n = 10) (Figure 2F). To avoid complication from the stimulus artifact, the IPSC and the [DA]<sub>o</sub> were instead compared at the time of the second voltammogram (165 ms post-stimulus). The D2-IPSC continued to lag behind the rise in the [DA]<sub>o</sub> such that the D2-IPSC had reached only  $53 \pm 8$  % (n = 10) of the maximum while the [DA]<sub>o</sub> had reached  $77 \pm 3$  % of the maximum (n = 10,  $p < 0.01$ , Student's paired *t* test) (Figures 2F and 2G). This indicates that the time required for metabotropic D2-receptor/G-protein/GIRK signaling likely limits the rate of activation of the IPSC.

### Vesicular Dopamine Release Activates D2-Receptor Mediated GIRK Currents

To examine the mechanisms underlying D2-receptor mediated synaptic transmission in MSNs, outward currents produced by evoked release were compared to those produced by the exogenous application of dopamine by iontophoresis. MSNs that displayed outward currents in response to exogenous dopamine also exhibited robust IPSCs (Figure 3A), indicating that neurons that responded to exogenous dopamine also formed functional synapses with dopamine terminals. Blockade of D2-receptors with sulpiride (500 nM, n = 7,  $p < 0.01$ , Student's paired *t* test) or GIRK channels with either Ba<sup>2+</sup> (200  $\mu$ M, n = 5,  $p < 0.001$ , Student's paired *t* test) or the GIRK channel blocker tertiapin-Q (300 nM, n = 5,  $p < 0.001$ , Student's paired *t* test) inhibited both the IPSC and the current produced by iontophoresis (Figures 3A and 3B), confirming that both conductances were the result of D2-receptor activation of GIRK channels. In contrast, inhibiting action potential firing with tetrodotoxin (TTX, 400 nM) or limiting presynaptic calcium entry with low extracellular calcium ACSF (no calcium added) blocked the D2-IPSC (n = 4 for both,  $p < 0.001$ , Student's paired *t* test) but failed to alter the amplitude of the current produced by iontophoresis (n = 4 for both,  $p > 0.3$ , Student's paired *t* test) (Figures 3A and 3B).

Reuptake by the dopamine transporter (DAT) regulates the [DA]<sub>o</sub> following release (Chen et al., 2006; Jones et al., 1998). To examine how DAT-mediated uptake limits the extent of D2-receptor activation during the IPSC, we blocked dopamine reuptake with the monoamine transport blocker cocaine. Cocaine (10  $\mu$ M) increased the amplitude (n = 7,  $p < 0.001$ , Student's paired *t* test) and duration (n = 7,  $p < 0.001$ , Student's paired *t* test) of D2-IPSCs (Figure 3C). This cocaine induced increase in IPSC amplitude was D2-receptor dependent as

it was blocked by subsequent addition of sulpiride (500 nM) ( $91 \pm 1\%$  inhibition,  $n = 8$ ,  $p < 0.001$ , Student's paired  $t$  test). Cocaine (1  $\mu$ M, 10  $\mu$ M) evoked a dose-dependent increase in the total charge transfer of IPSCs, measured as area under the curve (1  $\mu$ M:  $227 \pm 9\%$ ,  $n = 6$ ,  $p < 0.05$ ; 10  $\mu$ M:  $362 \pm 43\%$ ,  $n = 7$ ,  $p < 0.01$ , Student's paired  $t$  test) (Figure 3D). Cocaine also increased the GIRK current induced by exogenous application of dopamine (Figure S3A) but did not change the overall excitability of GIRK2<sup>+</sup> MSN as assessed by evoked AP firing (Figures S3B and S3C). Since the duration of receptor activation could be prolonged when reuptake was blocked, the results suggest that dopamine release evoked by a single stimulation only leads to the transient activation of D2-receptors.

Since MSNs receive inputs from multiple terminals that would be activated by electrical stimulation (Kreitzer, 2009; Lovinger, 2010), we confirmed that the D2-IPSC was the result of dopamine release from midbrain dopamine terminals in the striatum. The light-activated ion channel channelrhodopsin-2 (ChR2) was expressed in midbrain dopamine neurons by stereotaxic injection of an AAV coding for double-floxed ChR2-EYFP into the midbrain of tyrosine hydroxylase (TH)-Cre transgenic mice (Figures S3D–S3G). Wide-field illumination of the striatum with pulses of blue light (2 ms,  $\sim 1.0$  mW) evoked robust IPSCs in approximately half of GIRK2<sup>+</sup> MSNs examined (Figure 3E). IPSCs were abolished by sulpiride (500 nM) and the kinetics of light evoked currents were similar to those evoked by electrical stimulation (electrical: time to peak =  $262 \pm 15$  ms,  $n = 13$ ; optogenetic: time to peak =  $262 \pm 15$  ms,  $n = 13$ ,  $p = 0.9$ , Student's paired  $t$  test) (Figure 3E). FSCV was also used to measure [DA]<sub>o</sub> in response to optogenetic stimulation of ChR2-expressing dopamine terminals, confirming that a single wide-field pulse of blue light (2 ms) also produced a peak in the [DA]<sub>o</sub> ( $678 \pm 203$  nM,  $n = 9$ ) (Figure 3F).

### High Concentrations of Dopamine Are Required to Saturate Striatal D2-receptors

Pacemaker dopamine firing provides a background dopamine tone that is important for numerous striatal-dependent functions (Goto and Grace, 2008; Schultz, 2007b). As D2-receptors can exist in a high affinity state (Richfield et al., 1989), the nanomolar background dopamine tone has been hypothesized to maintain tonic activation of striatal D2-receptors *in vivo* (Floresco et al., 2003; Keefe et al., 1993; Schultz, 2007a; Surmeier et al., 2011). Given that we found that D2-receptors on MSNs encode phasic dopamine transients, we next examined how dopamine drives tonic D2-receptor mediated GIRK signaling.

As dopamine inputs to the striatum are cut in the brain slice, bath application of low concentrations of dopamine (1  $\mu$ M) was used as an initial attempt to mimic background tone. At 1  $\mu$ M, dopamine would be predicted to activate D2-receptors in the high-affinity state (Richfield et al., 1989). Surprisingly, dopamine at this concentration did not evoke a measurable outward current (baseline:  $11 \pm 8$  pA,  $n = 7$ ,  $p = 0.2$ , Student's paired  $t$  test) nor did it alter the amplitude of evoked D2-IPSCs (IPSC amplitude:  $94 \pm 5\%$  of control,  $n = 7$ ,  $p = 0.3$ , Student's paired  $t$  test) (Figures 4A – 4D). Subsequent application of a higher concentration (10  $\mu$ M), however, activated a standing outward GIRK current ( $31 \pm 8$  pA,  $n = 9$ ,  $p < 0.01$ , Student's paired  $t$  test), and also decreased the amplitude of D2-IPSCs ( $82 \pm 4\%$  of control,  $n = 9$ ,  $p < 0.01$ , Student's paired  $t$  test) (Figures 4A – 4D). Application of a saturating concentration of dopamine (100  $\mu$ M) produced a large current ( $79 \pm 18$  pA,  $n = 5$ ,

$p < 0.05$ , Student's paired  $t$  test) that now completely occluded the D2-IPSC ( $8 \pm 3\%$  of control,  $n = 5$ ,  $p < 0.001$ , Student's paired  $t$  test) (Figures 4A – 4D). The inhibition of the IPSC had an  $IC_{50}$  of  $36 \mu\text{M}$  (95% confidence interval =  $15 \mu\text{M}$  to  $58 \mu\text{M}$ ) and the dopamine mediated standing outward current had an  $EC_{50}$  of  $18 \mu\text{M}$  (95% confidence interval =  $9 \mu\text{M}$  to  $26 \mu\text{M}$ ) (Figures 4C and 4D).

As DAT-mediated uptake removes dopamine from the extracellular space, the effective concentration of dopamine that reaches the receptor within the slice may be less than the concentration in the bath. To increase penetration of dopamine into the slice, the same experiment was repeated in the presence of cocaine ( $10 \mu\text{M}$ ). The concentration-response curve for the inhibition of the IPSC was shifted to the left ( $IC_{50} = 9 \mu\text{M}$ , 95% confidence interval =  $5 \mu\text{M}$  to  $12 \mu\text{M}$ ) and dopamine evoked larger amplitude standing outward currents ( $100 \mu\text{M}$  dopamine:  $79 \pm 8 \text{ pA}$ ,  $n = 5$ ;  $100 \mu\text{M}$  dopamine in  $10 \mu\text{M}$  cocaine:  $190 \pm 35 \text{ pA}$ ,  $n = 7$ ,  $p < 0.05$ , Student's unpaired  $t$  test;  $EC_{50} = 16 \mu\text{M}$ , 95% confidence interval =  $7 \mu\text{M}$  to  $24 \mu\text{M}$ ) (Figures 4C and 4D). However, even in the presence of cocaine to block uptake, micromolar concentrations of dopamine were still required to produce sustained D2-receptor activation of GIRK channels. The results suggest that GIRK-coupled D2-receptors may preferentially exist in a low affinity state.

### GIRK Overexpression Does Not Affect the Affinity of Dopamine for D2-receptors

We next tested whether the high concentration of dopamine required to activate D2-receptors was a consequence of GIRK overexpression. In native GPCR-effector systems, the size of the effector pool often limits the maximal response (Kenakin, 2013; Ostrom et al., 2001). In order to determine whether the size of the expanded effector pool affected the affinity of dopamine for the D2-receptor, we limited the expression of GIRK by recording from MSNs 7 days after animals had been injected with AAV.

GIRK2 protein levels were initially quantified by western blot 7 and 24 days following AAV injection. GIRK2 expression increased by ~3-fold between the 7th and 24<sup>th</sup> day after AAV injection ( $n = 3$ ,  $p < 0.05$ , Student's paired  $t$  test) (Figures 5A and 5B). At 7 days post-injection, GIRK2 expression was 3-fold greater than control ( $3 \pm 1$  fold,  $n = 3$ ,  $p < 0.05$  vs. control hemisphere, Student's paired  $t$  test) while at 24 days GIRK2 levels were 10-fold greater than in the uninjected control hemisphere ( $10 \pm 1$  fold,  $n = 3$ ,  $p < 0.01$  vs. control hemisphere, Student's paired  $t$  test) (Figures 5A and 5B). To assess how differences in GIRK expression may affect the D2-IPSC, whole cell voltage clamp recordings were performed from GIRK2<sup>+</sup> MSNs in slices 7 days following injection of AAV (range: 5 to 9 days, mean = 7). Due to reduced expression of GIRK, D2-IPSCs were ~6-fold smaller in amplitude than control IPSCs recorded at least 21 days following injection (7 day post-injection:  $18 \pm 4 \text{ pA}$ ,  $n = 8$ ; > 21 days post-injection:  $102 \pm 5 \text{ pA}$ ,  $n = 130$ ,  $p < 0.001$ , Student's unpaired  $t$  test) (Figures 5C and 5D).

In brain slices taken from mice 7 days post-AAV injection, dopamine dose response measurements were repeated in the presence of  $10 \mu\text{M}$  cocaine (Figures 5C and 5D). Dopamine concentration-response curves for both the inhibition of the IPSC and the dopamine-induced outward current were constructed (Figures 5E and 5F). The inhibition of the IPSC in slices taken from animals 7-days post-injection had an  $IC_{50}$  of  $7 \mu\text{M}$  (95%

confidence interval = 6  $\mu$ M to 8  $\mu$ M) (Figure 5E), which was not different than the IC<sub>50</sub> for the inhibition of the IPSC in slices taken from animals greater than 21-days post injection (IC<sub>50</sub> = 9  $\mu$ M, 95% confidence interval = 5  $\mu$ M to 12  $\mu$ M), as indicated by their overlapping 95% confidence intervals. Likewise, there was no difference in the EC<sub>50</sub> of the dopamine-mediated standing outward current between MSNs following 7 or > 21 days of GIRK2 expression (7-day expression: 10  $\mu$ M, 95% confidence interval = 4  $\mu$ M to 16  $\mu$ M; > 21-day expression: 16  $\mu$ M, 95% confidence interval = 7  $\mu$ M to 24  $\mu$ M). The E<sub>max</sub> of D2-receptor activation, however, as measured as the size of the outward current produced by 100  $\mu$ M dopamine, was greater in mice with greater than 21-day expression (> 21-day expression: 190  $\pm$  36 pA, n = 7; 7-day expression: 27  $\pm$  6 pA, n = 11; p < 0.001, Student's unpaired *t* test) (Figure 5F). The results indicate that altering the size of the GIRK effector pool changes the maximum current evoked by dopamine but does not affect the potency of dopamine for the D2-receptor. Thus, despite differences in GIRK expression, there was no difference in the functional sensitivity of D2-receptor mediated currents.

### Transporters Regulate the Extent of D2-receptor Activation During Repetitive Stimulation

The kinetics of D2-IPSCs indicated that a single stimulation likely did not drive prolonged activation of D2-receptors. To examine if repetitive stimulation of dopamine terminals would lead to an increase in baseline D2-receptor activation, we repeatedly activated ChR2-expressing dopamine terminals using a 30 second train of optogenetic stimuli (1 Hz, 2 ms pulse) in an attempt to mimic tonic pacemaker firing of midbrain dopamine neurons. Recording from GIRK2<sup>+</sup> MSNs, light intensity was set such that the first evoked IPSC was roughly 50% maximum amplitude (~0.4 mW). This intensity of optogenetic stimulation produced a peak [DA]<sub>o</sub> of 191  $\pm$  19 nM (n = 8) for the first pulse and a steady state [DA]<sub>o</sub> (> 7 pulses after the initial pulse; 'plateau') of 61  $\pm$  11 nM (n = 8), as measured by FSCV (Figure 6A). This level of dopamine tone in the slice would be expected to activate D2-receptors in the high affinity state (Richfield et al., 1989). Despite the elevated background levels of dopamine in the extracellular space, each flash in the train reliably evoked an individual D2-IPSC (Figure 6B). Following an initial decline in the amplitude, IPSCs reached a stable amplitude of 24  $\pm$  5 pA (n = 15). Each D2-IPSC returned to a flat baseline before the next was initiated (Figure 6B, insert). No change in the baseline holding current was observed between each of the IPSCs in the train (1  $\pm$  1 pA, n = 15, p = 0.1, Student's one-sample *t* test) (Figures 6B and 6G), suggesting that the ~60 nM background level of dopamine in the slice that could be detected with FSCV (Figure 6A) did not lead to the tonic activation of D2-receptors. As the rate of GIRK activation is determined by the concentration of dopamine at the D2-receptor (Courtney and Ford, 2014; Ford et al., 2009), the fact that the rise times (10 – 90%) of IPSCs did not change over the course of the 30 second train (n = 9, p = 0.1, Pearson's correlation) (Figure 6C) suggests that each was the result of a similar sharp rise in a high concentration of dopamine.

Because DAT-mediated uptake determined the duration of D2-IPSCs evoked by a single stimulation (Figure 3C), we next sought to determine whether DATs limit persistent D2-receptor activation during repeated synaptic events. Cocaine (3  $\mu$ M) increased the steady state level of dopamine when measured with FSCV ('plateau' = 225  $\pm$  51 nM; n = 7, p < 0.001 versus control, Student's unpaired *t* test) (Figure 6A) and facilitated the amplitude and

duration of D2-IPSCs evoked during the train of optogenetic stimulation (Figure 6D). The duration of each IPSC was prolonged such that the next IPSC was initiated before the preceding synaptic current returned to baseline. This led to a change in the overall baseline between each oscillation (standing outward current:  $27 \pm 5$  pA,  $n = 13$ ,  $p < 0.001$  versus control, Student's unpaired  $t$  test) (Figure 6D), which increased the contribution of tonic signaling to the total amplitude of D2-receptor mediated standing outward current occurring during the train ( $57 \pm 5\%$ ,  $p < 0.001$ ,  $n = 13-15$ , Student's unpaired  $t$  test) (Figure 6E). Individual IPSCs could still be resolved superimposed on this standing outward current (Figure 6D, insert).

Since dopamine neuron pacemaker firing *in vivo* typically occurs in frequencies ranging from 3–8 Hz (Grace and Bunney, 1984a), we also increased the frequency of optogenetic stimulation during the 30-second train. In the absence of cocaine, increasing the frequency of stimulation of ChR2-expressing dopamine terminals to 2 Hz still resulted in small phasic D2-IPSCs (Figure 6F) but also induced a shift in the baseline holding current in between each oscillation (2 Hz optogenetic stimulation:  $16 \pm 5$  pA,  $n = 7$ ,  $p < 0.05$ , Student's one-sample  $t$  test) (Figures 6F and 6G). Subsequent stimulation at higher frequencies (5 Hz, Figure S3G) led to a summation of individual phasic D2-IPSCs such that only a sustained standing outward current could be observed ( $19 \pm 6$  pA,  $n = 11$ ,  $p < 0.01$ , Student's one-sample  $t$  test) (Figure 6F and 6G). These results indicate that at frequencies at least up to 2Hz, D2-receptors could encode the synaptic release of dopamine as individual signaling events.

### Tonic Extracellular Dopamine Does Not Occlude the D2-IPSC

As bath application of high concentrations of dopamine were required to drive large amplitude D2-receptor mediated outward currents (Figure 4D), it is likely that low concentrations of dopamine do not evoke full activation of D2-receptors on MSNs. To examine whether D2-receptors could differentially respond to a strong stimulation in the presence of tonic background activity, we again mimicked the pacemaker firing of dopamine neurons by repetitively stimulating ChR2-expressing dopamine terminals for several minutes (1 Hz, 2 ms pulse, light intensity set to ~50% maximum D2-IPSC amplitude). As above, repetitive optogenetic stimulation (1 Hz) evoked a series of D2-IPSCs that were entrained to the flashes of light for the duration of the experiment (Figure 7A). Following 2 minutes of optogenetic stimulation, a strong electrical stimulation was given to synchronously activate the majority of dopamine synaptic inputs to the MSN being recorded (stimulation intensity set to ~95% maximum). Despite background dopamine terminal stimulation for 2 minutes, the amplitude of the electrically evoked D2-IPSC was similar to control D2-IPSCs evoked prior to optogenetic stimulation (pre:  $92 \pm 9$  pA; during optogenetic stimulation:  $87 \pm 10$  pA;  $n = 7$ ,  $p = 0.4$ , Student's paired  $t$  test) (Figure 7B).

We repeated the same experiment across multiple stimulation frequencies to account for different dopamine neuron pacemaking frequencies (Grace and Bunney, 1984a). At 2 Hz and 5 Hz there was still no change in the amplitude of the electrically evoked IPSC (2 Hz optogenetic stimulation:  $94 \pm 5\%$  remaining after optogenetic stimulation,  $n = 5$ ,  $p = 0.4$ ; 5 Hz optogenetic stimulation:  $97 \pm 5\%$  remaining after optogenetic stimulation,  $n = 7$ ,  $p = 0.7$ ,

Student's paired *t* test) (Figures 7C and 7D). Even at the high frequency of 24 Hz, no occlusion of the IPSC was observed (Figure 7D). Instead, a small facilitation of the IPSC was seen ( $121 \pm 9\%$  increase in IPSC amplitude,  $n = 6$ ,  $p = 0.05$ , Student's paired *t* test). These results show that, in the brain slice, phasic D2-IPSCs could still be evoked in the presence of ambient dopamine resulting from tonic, pacemaker stimulation of dopamine terminals.

## Discussion

To date, the dynamics of striatal dopamine release have been widely studied using techniques that measure the extracellular concentration of dopamine (Chergui et al., 1994; Garris et al., 1994; Howe et al., 2013; Phillips et al., 2003). However, it has remained unclear how release events mediate post-synaptic dopamine receptor activation. In the present study, we introduced a potassium conductance to provide a new sensor of D2-receptor activation in MSNs. We found that IPSCs mediated by D2-receptor activation of GIRK channels occurred in under a second. These results indicate that D2-receptors are capable of encoding synaptic dopamine transients as distinct temporal events.

We found that following a single stimulation, the release of dopamine led to only a brief activation of D2-receptors. Activation of the GIRK conductance occurred with a rise time of 111 ms (10 – 90%) and lasted ~550 ms (20% width). As the extracellular dopamine transient that could be detected in the extracellular space occurred prior to the onset of the D2-IPSC, the time course of activation of the D2-IPSC was likely limited by the rate of activation of D2-receptor/G-protein/GIRK channels rather than the diffusion of dopamine from the release site. Due to the large size of the carbon fiber, FSCV samples bulk extracellular DA resulting from spillover from multiple release sites (Kawagoe et al., 1992). We found that the concentrations of dopamine required to drive GIRK currents and inhibit D2-IPSCs were higher than those detected by the carbon fiber following evoked release. As the concentration of DA decreases sharply as a function of distance away from the site of release (Cragg and Rice, 2004), the peak concentration of dopamine measured by the carbon fiber in the extracellular space is likely lower than the synaptic concentration present at D2-receptors mediating the IPSC. In isolated systems, only brief applications of saturating concentrations of agonists drive GPCR-coupled GIRK channel activation with similar kinetics to that seen during the D2-IPSC (Courtney and Ford, 2014; Ford et al., 2009; Sodickson and Bean, 1996). The activation of synaptic D2-receptors in MSNs underlying the IPSC therefore likely resulted from a sharp rise in the local concentration of dopamine.

At somatodendritic sites in the midbrain, the release of dopamine on to D2-receptors also drives a GIRK channel mediated IPSC (Beckstead et al., 2004). Despite differences in the anatomical location and mechanisms regulating the release of dopamine at axon terminals in the striatum and somatodendritic terminals in the midbrain (Schmitz et al., 2003), both IPSCs exhibited a remarkable similarity in their duration, kinetics, and dependence on uptake transporters for terminating their signaling (Beckstead et al., 2004; Ford et al., 2010). As individual vesicular release of dopamine is sufficient to drive the spontaneous activation of D2-receptors at somatodendritic synapses in the midbrain (Gantz et al., 2013), metabotropic transmission through the D2-receptor in multiple brain regions may involve a

more localized form of point-to-point signaling similar to that observed at ligand gated ion channel synapses.

Like other GPCRs, dopamine receptors can exist in multiple affinity states (Richfield et al., 1989; Sibley et al., 1982). According to the ternary complex model (De Lean et al., 1980), the high affinity state reflects the stabilized complex under guanine nucleotide-depleted conditions (Skinbjerg et al., 2012). In the presence of sodium and GTP, G-proteins uncouple from the receptor and the low affinity state is favored (Kenakin, 1996, 2013; Sibley et al., 1983). Since many of the biochemical binding assays that have classified dopamine D2-receptor affinity were done in membrane preparations in the absence of GTP, these measurements of affinity may differ from the functional state of the receptor in intact neurons (Sibley et al., 1983; Skinbjerg et al., 2012); van Wieringen et al., 2013). Both the high and low affinity states of the D2-receptor may be present in a given cell, but due to the high intracellular concentration of GTP, functionally coupled dopamine receptors in the low affinity state likely predominate (Castro et al., 2013; Ford et al., 2009; Schoffelmeer et al., 1994; Sibley et al., 1983).

In native GPCR systems, receptors, G-proteins and effectors have been estimated to exist in a ratio of ~1:200:3 (Post et al., 1995). Due to abundance of G-proteins, the pool of available effectors, not the receptors, often limits the maximal response (Ostrom et al., 2000). As such, past studies using membrane systems have shown that increases in the relative concentration of GPCRs leads to a shift in the concentration-response curve (Kenakin, 2013), while increased expression of effectors increases the efficacy without altering the functional affinity of agonists (Ostrom et al., 2001). In MSNs we found that the observed low affinity of dopamine for the D2-receptor was not dependent on the extent of GIRK expression. Examining the expression of GIRK over a 14 day period, we found that while there was a 3-fold increase in the amount of GIRK expression which corresponded to a 6-fold increase in the maximal effect of D2-receptor activation, there was no associated change in the EC<sub>50</sub>. Thus the low affinity state of the D2-receptor may play a larger functional role in striatal signaling in MSNs than previously thought.

As stimulatory D1-receptors are expressed on direct pathway MSNs and inhibitory D2-receptors are expressed on indirect pathway MSNs, dopamine is thought to maintain the balance between direct and indirect striatal activity in order to maintain appropriate output from the striatum (Albin et al., 1989; DeLong, 1990; Kravitz et al., 2010). Phasic dopamine events are proposed to signal the value of learned reward-predictive cues that drive motivated behavior (Schultz, 2007a). Based on studies of dopamine receptor affinity, it has been assumed that these dopamine transients primarily activate low affinity D1-receptors on the direct pathway. Our finding that striatal D2-receptors can respond to sub-second dopamine events suggests that these goal-directed actions may be driven, at least partially, by D2-receptor signaling in indirect pathway MSNs. Since dopamine terminals in the striatum exhibit dense axonal arborizations (Arbuthnott and Wickens, 2007; Matsuda et al., 2009), the firing of a single dopamine cell has been thought to provide dopamine tone to a large area encompassing many synapses. However, as we found that at low frequencies, stimulation of dopamine terminals evoked a series of IPSCs despite the extracellular basal tone of ~60 nM, local mechanisms may tightly limit the sphere of influence over which

dopamine signals at individual release sites. Over a range of stimulation frequencies, we found that robust D2-IPSCs could still be evoked superimposed on a dopamine mediated standing outward GIRK current when driven by a strong stimulus. Thus, despite the presence of baseline D2-receptor activation, phasic increases in the release of dopamine could still be differentially encoded in MSNs by D2-receptors.

D2-receptors are central to the etiology of many psychiatric diseases including schizophrenia (Howes and Kapur, 2009; Seeman et al., 2005) and current therapeutic approaches in the treatment of these diseases rely on global antagonism of this class of dopamine receptor. The unexpected finding that low affinity D2-receptors are activated by phasic dopamine transients raises the possibility for new pharmacological interventions that may specifically target the rapid interactions of dopamine with the D2-receptor.

## Experimental Procedures

### Stereotaxic injection

All animal procedures were performed in accordance with the guidelines of the Institutional Animal Care and Use Committee at Case Western Reserve University. Wild type C57BL6 or tyrosine hydroxylase (TH)::internal ribosomal entry site (IRES)-Cre heterozygote transgenic mice were injected at age P21. The coordinates for injection were (with respect to bregma), striatum: AP +1.2 mm, ML +1.8 mm, DV -3.35 mm; and substantia nigra pars compacta (SNc): AP -2.3 mm, ML +0.45 mm, DV -4.7 mm. Virus was injected via a pulled pipette using a Nanoject II (Drummond Scientific). For striatal injections, a total volume of 300 nL of AAV2/9.hSynapsin.tdTomato.T2A.mGIRK2-1-A22A.WPRE (Vollum Viral Core, Oregon Health Science University) was injected. In a few cases as noted (Figure S1), AAV2/9.hSynapsin.tdTomato.T2A.mGIRK2-1-A22A.WPRE was mixed with AAV2/9.hSynapsin.eGFP.T2A.ratGIRK1-A32A.WPRE (Vollum Viral Core, Oregon Health Science University). For SNc injections, 500 nL of AAV5.EF1a.DIO.hChR2(H134R)-EYFP.WPRE.hGH (University of Pennsylvania Viral Core) or AAV9.CAG.hChR2(H134R).mCherry.WPRE.SV40 (University of Pennsylvania Viral Core) was injected into the SNc of TH-Cre transgenic or wild type C57BL6 mice, respectively. No difference was observed in the kinetics of light-evoked D2-IPSCs between the two different ChR2 AAVs (time to peak:  $n = 16-17$ ,  $p = 0.2$ ). Animals recovered for ~3-4 weeks to allow for expression.

### Immunohistochemistry

AAV2/9.hSynapsin.tdTomato.T2A.mGIRK2-1-A22A.WPRE-injected mice were deeply anesthetized with an i.p. injection of avertin (250 mg/kg). Mice were transcardially perfused with ice-cold phosphate-buffered saline (PBS) containing (in mM) 137 NaCl, 1.5  $\text{KH}_2\text{PO}_4$ , 8  $\text{NaH}_2\text{PO}_4$ , 2.7 KCl (pH = 7.4), followed by 4% paraformaldehyde in PBS. The brains were fixed overnight in 4% paraformaldehyde. Fixed brains were sectioned coronally in 25  $\mu\text{m}$  sections. Free-floating sections were permeabilized with 0.2% Triton X-100 in PBS (PBS-T) and blocked in 5% normal goat serum in PBS-T for one hour at room temperature. Slices were washed and incubated with 1:500 polyclonal rabbit anti-Kir3.2 antibodies (Alomone) in PBS overnight at 4°C. Sections were incubated with 1:500 Alexa 647-

conjugated goat-anti-rabbit IgG (Invitrogen) in PBS for 2 hours at room temperature. Slices were mounted onto microscope slides (Fisher Scientific). Fluorescent confocal images were obtained using a Zeiss LSM 510 META laser scanning confocal microscope (Carl Zeiss) with a 40x Plan-Neofluar, NA 1.3, oil-immersion lens. All images were processed using ImageJ.

### Western blots

The striatum was dissected from control and GIRK2-injected hemispheres of mice 7 days and 24 days following AAV injection. Tissue was homogenized in tissue homogenization buffer (250 mM sucrose, 20 mM Tris-HCl pH 7.4, 1 mM EDTA, 1 mM EGTA) containing Protease Inhibitor Cocktail (Sigma) and sonicated. Protein concentrations were quantified by Pierce BCA (Thermo Scientific). Equivalent amounts of protein were loaded into a 10% SDS gel and resolved by SDS-PAGE. Protein was transferred to a PVDF membrane, blocked with 5% milk in TBS-T (0.1% Tween), and probed with anti-GIRK2 (Alomone) or anti-GAPDH (Santa Cruz Biotechnology). Blots were probed with appropriate secondary antibody conjugated to HRP (GE Healthcare). Proteins were visualized with enhanced chemiluminescence (Millipore). Densitometry was performed with ImageJ and GIRK2 protein levels were normalized to GAPDH.

### Slice preparation

Coronal slices (240  $\mu$ m) containing the striatum were made in ice-cold physiological saline solution containing (in mM): 75 NaCl, 2.5 KCl, 6 MgCl<sub>2</sub>, 0.1 CaCl<sub>2</sub>, 1.2 NaH<sub>2</sub>PO<sub>4</sub>, 25 NaHCO<sub>3</sub>, 2.5 D-glucose, and 50 sucrose. Slices were incubated at 35°C for at least 45 minutes in ACSF containing (in mM) 126 NaCl, 2.5 KCl, 1.2 MgCl<sub>2</sub>, 2.5 CaCl<sub>2</sub>, 1.2 NaHPO<sub>4</sub>, 21.4 NaHCO<sub>3</sub>, 11.1 D-glucose and 10  $\mu$ M MK-801 while being bubbled with 95% O<sub>2</sub> and 5% CO<sub>2</sub>. Following incubation, slices were placed in a recording chamber and were constantly perfused with ACSF (34  $\pm$  2°C) at 2 ml/min. ACSF contained 100  $\mu$ M picrotoxin, 10  $\mu$ M DNQX, 300 nM CGP55845, 200 nM scopolamine hydrobromide, and 1  $\mu$ M SCH 23390 hydrochloride to isolate D2-receptor-mediated currents. Medium spiny neurons (MSNs) were visualized with a BXWI51 microscope (Olympus) with infrared gradient contrast optics. tdTomato was visualized by fluorescence using an LED (Thorlabs).

### Electrophysiology

Whole-cell voltage clamp recordings were made from fluorescent (tdTomato<sup>+</sup>, GIRK2<sup>+</sup>) MSNs using an Axopatch 200B amplifier (Molecular Devices) and acquired with Axograph X (Axograph Scientific) at 10 kHz and filtered to 2 kHz. Patch pipettes (1.5–2 M $\Omega$ ) (World Precision Instruments) contained 115 mM K-methylsulphate, 20 mM NaCl, 1.5 mM MgCl<sub>2</sub>, 10 mM HEPES(K), 10 mM BAPTA-tetrapotassium, 1 mg/ml ATP, 0.1 mg/ml GTP, and 1.5 mg/ml phosphocreatine (pH 7.4, 275 mOsm). GIRK2<sup>+</sup> MSNs were held at –60 mV. No series resistance compensation was used and cells were discarded if the access resistance rose above 15 M $\Omega$ .

Electrical stimulation was used to evoke dopamine release using a monopolar ACSF-filled extracellular glass stimulating electrode. A single stimulation (0.7 ms, 20 – 50  $\mu$ A) was used to evoke release from dopamine terminals in the striatum. Light-evoked dopamine release

was elicited by stimulating ChR2 with widefield 488 nm blue light (pulse width = 2 ms) through the objective via a white light LED (Thorlabs) filtered with a FITC bandpass filter set (460–495 nm; Chroma) (0.2–1.0 mW/mm<sup>2</sup>). Drugs were applied by bath perfusion. Quinpirole was applied either through a puffing pipette containing quinpirole (100 μM) with a Picospritzer II (General Valve Corporation) or by bath application. Dopamine was bath applied or iontophoresed via a thin-walled iontophoretic glass electrode that was loaded with 1M dopamine and placed ~10 μm from the soma of the cell being recorded. Dopamine was ejected as a cation (160 nA) for 1 s for maximum dopamine currents or in 20–50 ms pulses for stable iontophoretic currents (1 pulse/min). Leakage of dopamine was prevented with a retention current of 3–20 nA.

### Fast scan cyclic voltammetry (FSCV)

Electrochemical recordings were made using carbon fiber electrodes (34–700, Goodfellow) encased within a glass pipette. Electrodes had an exposed diameter of 7 μm and length of 50–100 μm. The carbon fiber tip was soaked in activated carbon purified isopropanol for 20 – 30 minutes prior to use. The tip of the fiber was placed in striatum 30 – 70 μm below the surface of the slice. The fiber was held at –0.4 V, and triangular waveforms (–0.4 to 1.3 V vs. Ag/AgCl at 400 V/S) were applied at 10 Hz. Background subtracted cyclic voltammogram currents were obtained by subtracting the average of 10 voltammograms obtained prior to stimulation from each voltammogram obtained after stimulation. The time course of dopamine was determined by plotting their peak oxidation potentials versus time. After experimentation, each electrode was calibrated against known concentrations of dopamine. In all cases the stimulation intensity and duration used to evoke dopamine release used was the same as in electrophysiological experiments.

### Materials

Picrotoxin, DNQX, and MK-801 were obtained from Ascent Scientific. CGP 55845, scopolamine hydrobromide, SCH 23390, S-(–)-sulpiride and tertiapin-Q were from Tocris Bioscience. K-methylsulphate was from Acros Organic and BAPTA was from Invitrogen. Cocaine hydrochloride was obtained from the National Institute of Drug Abuse. All other chemicals were from Sigma-Aldrich.

### Statistics and analysis

Data are shown as mean ± SEM. Statistical significance was determined using a one-way ANOVA, Pearson's correlation, or a Student's paired or unpaired t-test, as appropriate (InStat 3.0, Graphpad). Statistical significance was defined as  $p < 0.05$  (\*),  $p < 0.01$  (\*\*), and  $p < 0.001$  (\*\*\*). Activation kinetics of the D2-IPSC were analyzed by subtracting traces recorded in the presence of sulpiride from traces containing D2-IPSCs to blank the stimulation artifact.

### Supplementary Material

Refer to Web version on PubMed Central for supplementary material.

## Acknowledgments

This work was funded by NIH grants R00-DA26417, R01-DA35821, a NARSAD Young Investigator Grant and a Mt. Sinai Health Care Foundation Scholars Award to CPF, and NIH T32 grant GM007250 to PFM.

We thank Chris Bond and Eric Washburn for viral vectors, Michael Bruchas for providing TH-Cre mice, Bryan Luikart, Steven Wyler and Evan Deneris for sequencing and molecular assistance, Colleen Karlo and Samantha Barclay for technical assistance, and Ben Strowbridge and John Williams for helpful comments on the manuscript.

## References

- Albin RL, Young AB, Penney JB. The functional anatomy of basal ganglia disorders. *Trends Neurosci.* 1989; 12:366–375. [PubMed: 2479133]
- Arbuthnott GW, Wickens J. Space, time and dopamine. *Trends Neurosci.* 2007; 30:62–69. [PubMed: 17173981]
- Baik JH, Picetti R, Saiardi A, Thiriet G, Dierich A, Depaulis A, Le Meur M, Borrelli E. Parkinsonian-like locomotor impairment in mice lacking dopamine D2 receptors. *Nature.* 1995; 377:424–428. [PubMed: 7566118]
- Beckstead MJ, Grandy DK, Wickman K, Williams JT. Vesicular dopamine release elicits an inhibitory postsynaptic current in midbrain dopamine neurons. *Neuron.* 2004; 42:939–946. [PubMed: 15207238]
- Berke JD, Hyman SE. Addiction, dopamine, and the molecular mechanisms of memory. *Neuron.* 2000; 25:515–532. [PubMed: 10774721]
- Bromberg-Martin ES, Hikosaka O. Midbrain dopamine neurons signal preference for advance information about upcoming rewards. *Neuron.* 2009; 63:119–126. [PubMed: 19607797]
- Castro LR, Brito M, Guiot E, Polito M, Korn CW, Herve D, Girault JA, Paupardin-Tritsch D, Vincent P. Striatal neurones have a specific ability to respond to phasic dopamine release. *J Physiol.* 2013; 591:3197–3214. [PubMed: 23551948]
- Chen R, Tilley MR, Wei H, Zhou F, Zhou FM, Ching S, Quan N, Stephens RL, Hill ER, Nottoli T, et al. Abolished cocaine reward in mice with a cocaine-insensitive dopamine transporter. *Proc Natl Acad Sci U S A.* 2006; 103:9333–9338. [PubMed: 16754872]
- Chergui K, Suaud-Chagny MF, Gonon F. Nonlinear relationship between impulse flow, dopamine release and dopamine elimination in the rat brain in vivo. *Neuroscience.* 1994; 62:641–645. [PubMed: 7870295]
- Courtney NA, Ford CP. The timing of dopamine- and noradrenaline-mediated transmission reflects underlying differences in the extent of spillover and pooling. *J Neurosci.* 2014; 34:7645–7656. [PubMed: 24872568]
- Cragg S, Rice ME, Greenfield SA. Heterogeneity of electrically evoked dopamine release and reuptake in substantia nigra, ventral tegmental area, and striatum. *J Neurophysiol.* 1997; 77:863–873. [PubMed: 9065855]
- Cragg SJ, Rice ME. Dancing past the DAT at a DA synapse. *Trends Neurosci.* 2004; 27:270–277. [PubMed: 15111009]
- De Lean A, Stadel JM, Lefkowitz RJ. A ternary complex model explains the agonist-specific binding properties of the adenylate cyclase-coupled beta-adrenergic receptor. *The Journal of biological chemistry.* 1980; 255:7108–7117. [PubMed: 6248546]
- DeLong MR. Primate models of movement disorders of basal ganglia origin. *Trends Neurosci.* 1990; 13:281–285. [PubMed: 1695404]
- Floresco SB, West AR, Ash B, Moore H, Grace AA. Afferent modulation of dopamine neuron firing differentially regulates tonic and phasic dopamine transmission. *Nat Neurosci.* 2003; 6:968–973. [PubMed: 12897785]
- Ford CP, Gantz SC, Phillips PE, Williams JT. Control of extracellular dopamine at dendrite and axon terminals. *J Neurosci.* 2010; 30:6975–6983. [PubMed: 20484639]
- Ford CP, Phillips PE, Williams JT. The time course of dopamine transmission in the ventral tegmental area. *J Neurosci.* 2009; 29:13344–13352. [PubMed: 19846722]

- Gantz SC, Bunzow JR, Williams JT. Spontaneous inhibitory synaptic currents mediated by a G protein-coupled receptor. *Neuron*. 2013; 78:807–812. [PubMed: 23764286]
- Garris PA, Ciolkowski EL, Pastore P, Wightman RM. Efflux of dopamine from the synaptic cleft in the nucleus accumbens of the rat brain. *J Neurosci*. 1994; 14:6084–6093. [PubMed: 7931564]
- Gerfen CR, Surmeier DJ. Modulation of striatal projection systems by dopamine. *Annual review of neuroscience*. 2011; 34:441–466.
- Goto Y, Grace AA. Limbic and cortical information processing in the nucleus accumbens. *Trends Neurosci*. 2008; 31:552–558. [PubMed: 18786735]
- Grace AA, Bunney BS. The Control of Firing Pattern in Nigral Dopamine Neurons - Single Spike Firing. *Journal of Neuroscience*. 1984a; 4:2866–2876. [PubMed: 6150070]
- Grace AA, Bunney BS. The control of firing pattern in nigral dopamine neurons: burst firing. *J Neurosci*. 1984b; 4:2877–2890. [PubMed: 6150071]
- Grace AA, Floresco SB, Goto Y, Lodge DJ. Regulation of firing of dopaminergic neurons and control of goal-directed behaviors. *Trends Neurosci*. 2007; 30:220–227. [PubMed: 17400299]
- Graybiel AM. Neurotransmitters and neuromodulators in the basal ganglia. *Trends Neurosci*. 1990; 13:244–254. [PubMed: 1695398]
- Hoffman AF, Gerhardt GA. Differences in pharmacological properties of dopamine release between the substantia nigra and striatum: an in vivo electrochemical study. *J Pharmacol Exp Ther*. 1999; 289:455–463. [PubMed: 10087038]
- Howe MW, Tierney PL, Sandberg SG, Phillips PE, Graybiel AM. Prolonged dopamine signalling in striatum signals proximity and value of distant rewards. *Nature*. 2013; 500:575–579. [PubMed: 23913271]
- Howes OD, Kapur S. The dopamine hypothesis of schizophrenia: version III--the final common pathway. *Schizophr Bull*. 2009; 35:549–562. [PubMed: 19325164]
- Jones SR, Gainetdinov RR, Jaber M, Giros B, Wightman RM, Caron MG. Profound neuronal plasticity in response to inactivation of the dopamine transporter. *Proc Natl Acad Sci U S A*. 1998; 95:4029–4034. [PubMed: 9520487]
- Karschin C, Dissmann E, Stuhmer W, Karschin A. IRK(1–3) and GIRK(1–4) inwardly rectifying K<sup>+</sup> channel mRNAs are differentially expressed in the adult rat brain. *J Neurosci*. 1996; 16:3559–3570. [PubMed: 8642402]
- Kawagoe KT, Garris PA, Wiedemann DJ, Wightman RM. Regulation of transient dopamine concentration gradients in the microenvironment surrounding nerve terminals in the rat striatum. *Neuroscience*. 1992; 51:55–64. [PubMed: 1465186]
- Kawaguchi Y, Wilson CJ, Augood SJ, Emson PC. Striatal interneurons: chemical, physiological and morphological characterization. *Trends Neurosci*. 1995; 18:527–535. [PubMed: 8638293]
- Keefe KA, Zigmond MJ, Abercrombie ED. In vivo regulation of extracellular dopamine in the neostriatum: influence of impulse activity and local excitatory amino acids. *Journal of neural transmission General section*. 1993; 91:223–240. [PubMed: 8099798]
- Kenakin T. The classification of seven transmembrane receptors in recombinant expression systems. *Pharmacol Rev*. 1996; 48:413–463. [PubMed: 8888308]
- Kenakin T. New concepts in pharmacological efficacy at 7TM receptors: IUPHAR review 2. *Br J Pharmacol*. 2013; 168:554–575. [PubMed: 22994528]
- Kita T, Kita H, Kitai ST. Passive electrical membrane properties of rat neostriatal neurons in an in vitro slice preparation. *Brain Res*. 1984; 300:129–139. [PubMed: 6329425]
- Kobayashi T, Ikeda K, Ichikawa T, Abe S, Togashi S, Kumanishi T. Molecular cloning of a mouse G-protein-activated K<sup>+</sup> channel (mGIRK1) and distinct distributions of three GIRK (GIRK1, 2 and 3) mRNAs in mouse brain. *Biochem Biophys Res Commun*. 1995; 208:1166–1173. [PubMed: 7702616]
- Kravitz AV, Freeze BS, Parker PR, Kay K, Thwin MT, Deisseroth K, Kreitzer AC. Regulation of parkinsonian motor behaviours by optogenetic control of basal ganglia circuitry. *Nature*. 2010; 466:622–626. [PubMed: 20613723]
- Kreitzer AC. Physiology and pharmacology of striatal neurons. *Annual review of neuroscience*. 2009; 32:127–147.

- Lesage F, Guillemare E, Fink M, Duprat F, Heurteaux C, Fosset M, Romey G, Barhanin J, Lazdunski M. Molecular properties of neuronal G-protein-activated inwardly rectifying K<sup>+</sup> channels. *The Journal of biological chemistry*. 1995; 270:28660–28667. [PubMed: 7499385]
- Liao YJ, Jan YN, Jan LY. Heteromultimerization of G-protein-gated inwardly rectifying K<sup>+</sup> channel proteins GIRK1 and GIRK2 and their altered expression in weaver brain. *J Neurosci*. 1996; 16:7137–7150. [PubMed: 8929423]
- Lovinger DM. Neurotransmitter roles in synaptic modulation, plasticity and learning in the dorsal striatum. *Neuropharmacology*. 2010; 58:951–961. [PubMed: 20096294]
- Luscher C, Slesinger PA. Emerging roles for G protein-gated inwardly rectifying potassium (GIRK) channels in health and disease. *Nat Rev Neurosci*. 2010; 11:301–315. [PubMed: 20389305]
- Matsuda W, Furuta T, Nakamura KC, Hioki H, Fujiyama F, Arai R, Kaneko T. Single nigrostriatal dopaminergic neurons form widely spread and highly dense axonal arborizations in the neostriatum. *J Neurosci*. 2009; 29:444–453. [PubMed: 19144844]
- Meisenzahl EM, Schmitt GJ, Scheuerecker J, Moller HJ. The role of dopamine for the pathophysiology of schizophrenia. *Int Rev Psychiatry*. 2007; 19:337–345. [PubMed: 17671867]
- Nicola SM, Malenka RC. Modulation of synaptic transmission by dopamine and norepinephrine in ventral but not dorsal striatum. *J Neurophysiol*. 1998; 79:1768–1776. [PubMed: 9535946]
- Ostrom RS, Gregorian C, Drenan RM, Xiang Y, Regan JW, Insel PA. Receptor number and caveolar co-localization determine receptor coupling efficiency to adenylyl cyclase. *The Journal of biological chemistry*. 2001; 276:42063–42069. [PubMed: 11533056]
- Ostrom RS, Post SR, Insel PA. Stoichiometry and compartmentation in G protein-coupled receptor signaling: implications for therapeutic interventions involving G(s). *J Pharmacol Exp Ther*. 2000; 294:407–412. [PubMed: 10900212]
- Phillips PE, Stuber GD, Heien ML, Wightman RM, Carelli RM. Subsecond dopamine release promotes cocaine seeking. *Nature*. 2003; 422:614–618. [PubMed: 12687000]
- Post SR, Hilal-Dandan R, Urasawa K, Brunton LL, Insel PA. Quantification of signalling components and amplification in the beta-adrenergic-receptor-adenylate cyclase pathway in isolated adult rat ventricular myocytes. *The Biochemical journal*. 1995; 311(Pt 1):75–80. [PubMed: 7575483]
- Richfield EK, Penney JB, Young AB. Anatomical and affinity state comparisons between dopamine D1 and D2 receptors in the rat central nervous system. *Neuroscience*. 1989; 30:767–777. [PubMed: 2528080]
- Schmitz Y, Benoit-Marand M, Gonon F, Sulzer D. Presynaptic regulation of dopaminergic neurotransmission. *J Neurochem*. 2003; 87:273–289. [PubMed: 14511105]
- Schoffelmeer AN, Hogenboom F, Mulder AH, Ronken E, Stoof JC, Drukarch B. Dopamine displays an identical apparent affinity towards functional dopamine D1 and D2 receptors in rat striatal slices: possible implications for the regulatory role of D2 receptors. *Synapse*. 1994; 17:190–195. [PubMed: 7974202]
- Schultz W. Behavioral dopamine signals. *Trends Neurosci*. 2007a; 30:203–210. [PubMed: 17400301]
- Schultz W. Multiple dopamine functions at different time courses. *Annual review of neuroscience*. 2007b; 30:259–288.
- Seeman P, Weinshenker D, Quirion R, Srivastava LK, Bhardwaj SK, Grandy DK, Premont RT, Sotnikova TD, Boksa P, El-Ghundi M, et al. Dopamine supersensitivity correlates with D2High states, implying many paths to psychosis. *Proc Natl Acad Sci U S A*. 2005; 102:3513–3518. [PubMed: 15716360]
- Sibley DR, De Lean A, Creese I. Anterior pituitary dopamine receptors. Demonstration of interconvertible high and low affinity states of the D-2 dopamine receptor. *The Journal of biological chemistry*. 1982; 257:6351–6361. [PubMed: 6176582]
- Sibley DR, Mahan LC, Creese I. Dopamine receptor binding on intact cells. Absence of a high-affinity agonist-receptor binding state. *Mol Pharmacol*. 1983; 23:295–302. [PubMed: 6835198]
- Skinbjerg M, Sibley DR, Javitch JA, Abi-Dargham A. Imaging the high-affinity state of the dopamine D2 receptor in vivo: fact or fiction? *Biochemical pharmacology*. 2012; 83:193–198. [PubMed: 21945484]
- Sodickson DL, Bean BP. GABAB receptor-activated inwardly rectifying potassium current in dissociated hippocampal CA3 neurons. *J Neurosci*. 1996; 16:6374–6385. [PubMed: 8815916]

- Surmeier, DJ. Striatum: Cell Types, Membrane Properties and Neuromodulation; Microcircuits in the striatum. Cambridge, MA: The MIT Press; 2006.
- Surmeier DJ, Carrillo-Reid L, Bargas J. Dopaminergic modulation of striatal neurons, circuits, and assemblies. *Neuroscience*. 2011; 198:3–18. [PubMed: 21906660]
- Tepper, JMPD. Striatum: Striatal Cell Types and their Interaction. In: Graybiel, G., editor. *Microcircuits: The interface between neurons and global brain function*. Cambridge, MA: The MIT Press; 2006. p. 127-148.
- Tobler PN, Fiorillo CD, Schultz W. Adaptive coding of reward value by dopamine neurons. *Science*. 2005; 307:1642–1645. [PubMed: 15761155]
- Tritsch NX, Sabatini BL. Dopaminergic modulation of synaptic transmission in cortex and striatum. *Neuron*. 2012; 76:33–50. [PubMed: 23040805]
- Volkow ND, Fowler JS, Wang GJ, Baler R, Telang F. Imaging dopamine's role in drug abuse and addiction. *Neuropharmacology*. 2009; 56(Suppl 1):3–8. [PubMed: 18617195]
- Wightman RM, Kuhr WG, Ewing AG. Voltammetric detection of dopamine release in the rat corpus striatum. *Ann N Y Acad Sci*. 1986; 473:92–105. [PubMed: 3541742]

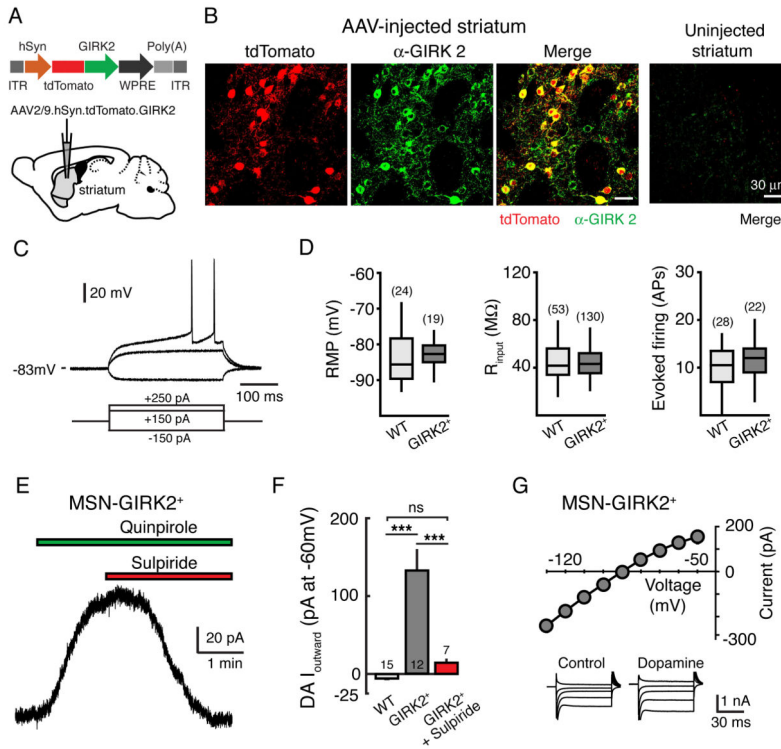


**Figure 1. Expression of GIRK2 in MSNs**

(A) Schematic of AAV2/9.hSyn.tdTomato.T2A.GIRK2.WPRE vector injection into the striatum. (B) AAV induced expression of GIRK2 and tdTomato in striatal sections three weeks following injection. Shown are tdTomato fluorescence (left), GIRK2 immunoreactivity (middle), and co-localization (right) panels. No tdTomato fluorescence or GIRK2 immunoreactivity could be detected above background levels from the contralateral uninjected hemisphere (far right, merged). Scale bar equals 30  $\mu\text{m}$  for all panels. (C) Current-clamp recording from a GIRK2<sup>+</sup> MSN. Membrane responses to +250, +150 and -150 pA current injections. (D) No differences were found in the passive membrane properties between WT control MSNs and GIRK2<sup>+</sup> MSNs. Left: resting membrane potential (RMP); middle: membrane input resistance ( $R_{\text{input}}$ ); right: MSN firing rate (number of action potentials (APs) evoked by 450 pA current injection, 300 ms). Data median and first and third quartiles are shown as box plots. (E) Example trace from a GIRK2<sup>+</sup> MSN. Bath application of the D2-agonist quinpirole (1  $\mu\text{M}$ ) evokes an outward current that is reversed by the D2-antagonist sulpiride (500 nM). (F) Summary data illustrating the maximum outward current in response to the iontophoretic application of dopamine in WT control MSNs, GIRK2<sup>+</sup> MSNs, and GIRK2<sup>+</sup> MSNs in the presence of sulpiride (500 nM). (G) DA-evoked current-voltage relationship. 10 mV voltage steps were given from -50 mV to -130 mV. Inserts depict representative traces (shown in 20 mV increments for clarity) under control conditions and in the presence of dopamine. Subtraction of the control traces from those in the presence of dopamine reveals a conductance that reverses near the predicted potassium reversal potential ( $n = 6$ ). \*\*\* =  $p < 0.001$  by one-way ANOVA with Tukey Kramer post-hoc test. Error bars indicate  $\pm$  SEM. Numbers in bar graphs represent number of cells recorded. See also Figure S1.

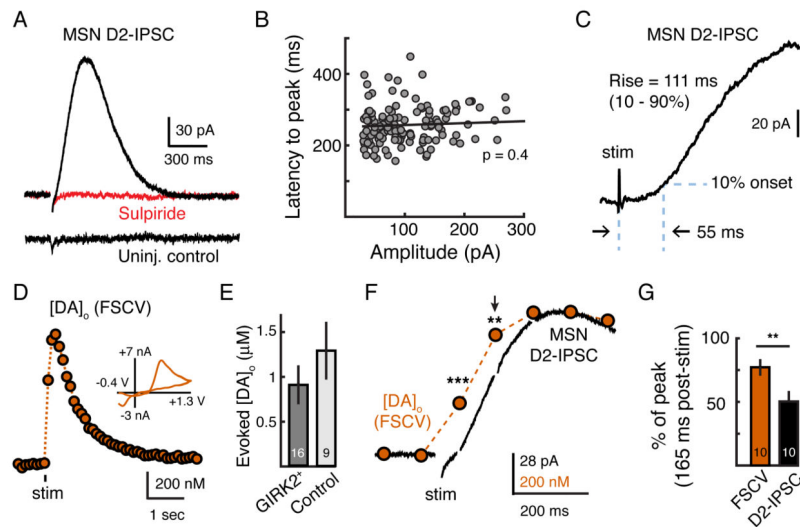


**Figure 2. Phasic Dopamine Transients Drive D2-IPSCs**

(A) Representative whole-cell recording of a  $GIRK2^+$  MSN (top) and a control MSN from the uninjected hemisphere (bottom). A single electrical stimulation evokes an IPSC that is blocked by the D2-antagonist sulpiride ( $1 \mu\text{M}$ ) (top). No IPSC could be evoked in MSNs from uninjected control hemispheres (bottom). (B) Latency to peak does not correlate with amplitude of the D2-IPSC (Pearson’s correlation). Circles represent IPSCs recorded from individual  $GIRK2^+$  MSNs ( $n = 130$ ). (C) Whole-cell recordings made in the presence of sulpiride ( $1 \mu\text{M}$ ) were subtracted from recordings of D2-IPSCs to blank the stimulation artifact and quantify activation kinetics ( $n = 20$ ). IPSCs exhibited a lag of  $55 \pm 3$  ms prior to reaching 10% of the peak amplitude, and had rise times (10 – 90%) of  $111 \pm 6$  ms ( $n = 20$ ). (D) Representative FSCV trace measuring the  $[\text{DA}]_o$  from a control striatal brain slice in response to a single stimulation. Inset shows the cyclic voltammogram produced by a triangular waveform ( $-0.4$  V to  $+1.3$  V,  $400$  V/s). (E) Summary of the  $[\text{DA}]_o$  evoked (measured by FSCV) following a single stimulation. Slices used were taken from animals three weeks following AAV.GIRK2 injection and wild type controls. (F) Simultaneous whole-cell recording of a  $GIRK2^+$  MSN (black) and FSCV (orange) scaled to the peak. FSCV waveform artifacts in the electrophysiological trace were blanked. Arrow indicates time point (165 ms post-stimulus) used for quantification in G. (G) Summary data showing that the D2-IPSC lags behind the  $[\text{DA}]_o$  ( $n = 10$ ). Presented as the percent of the peak at the second voltammogram (165 ms) after stimulation. Error bars indicate  $\pm$  SEM. \*\* =  $p < 0.01$ , \*\*\* =  $p < 0.001$  by Student’s paired  $t$  test. See also Figure S2.

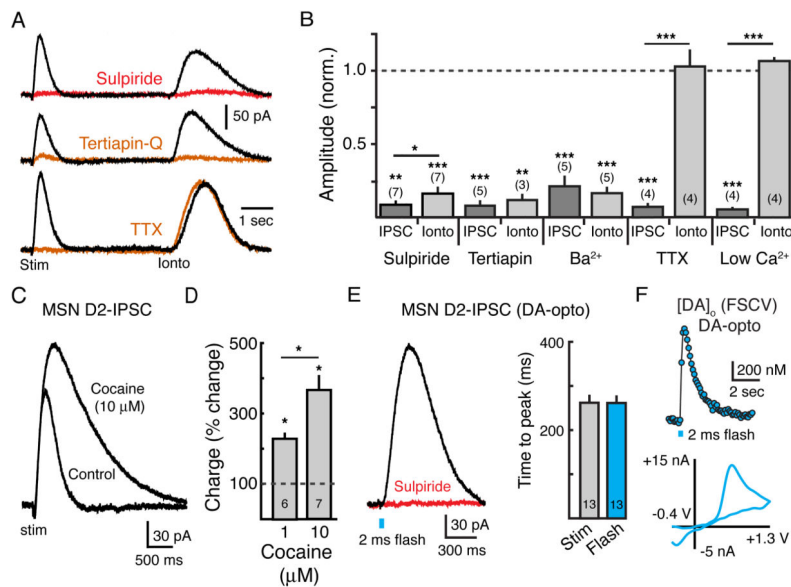


**Figure 3. Synaptic Activation of MSN D2-receptors Is Regulated by Uptake**

(A) Representative traces illustrating D2-IPSCs evoked with a single stimulation followed by outward currents evoked by iontophoretic application of exogenous dopamine (160 nA, 20–50 ms) under control conditions (black), and in the presence of the D2-antagonist sulpiride (500 nM, top trace, red), the inward-rectifier potassium channel blocker tertiapin-Q (300 nM, middle trace, orange), and the voltage-gated sodium channel blocker tetrodotoxin (TTX, 600 nM, bottom trace, orange). (B) Summary data showing the normalized amplitude of both the D2-IPSC and the current evoked by DA-iontophoresis in different experiments in the presence of sulpiride (500 nM), tertiapin Q (300 nM), Ba<sup>2+</sup> (200 μM), low Ca<sup>2+</sup> (0 mM added) and TTX (400 nM). (C) Representative whole-cell recording under control conditions and in the presence of the DAT-inhibitor cocaine (10 μM), illustrating the role of transporters in regulating the time course of transmission. (D) Summary data showing the normalized percent increase in total charge (area under the curve: pA/ms) of the IPSC in 1 μM (n = 6, p < 0.05) and 10 μM (n = 7, p < 0.05) cocaine. (E) Optogenetic activation of ChR2-expressing dopamine terminals in the striatum evokes a D2-IPSC in GIRK2<sup>+</sup> MSNs. Left panel: representative trace showing that the light-evoked IPSC is blocked by the D2-antagonist sulpiride (500 nM). Flash duration was 2 ms (~1.0 mW). Right panel: Summary data demonstrating similar time courses of electrically and optogenetically evoked D2-IPSCs (n = 13, p = 0.9). (F) Representative FSCV trace showing [DA]<sub>o</sub> in response to optogenetic stimulation of ChR2-expressing dopamine terminals (2 ms flash). Lower panel: cyclic voltammogram produced by a triangular waveform (–0.4 V to +1.3 V, 400 V/s) following optogenetic stimulation of dopamine terminals. Error bars indicate ± SEM. \* = p < 0.05, \*\* = p < 0.01, \*\*\* = p < 0.001 by Student’s *t* test. Numbers in bar graphs represent number of cells recorded. See also Figure S3.

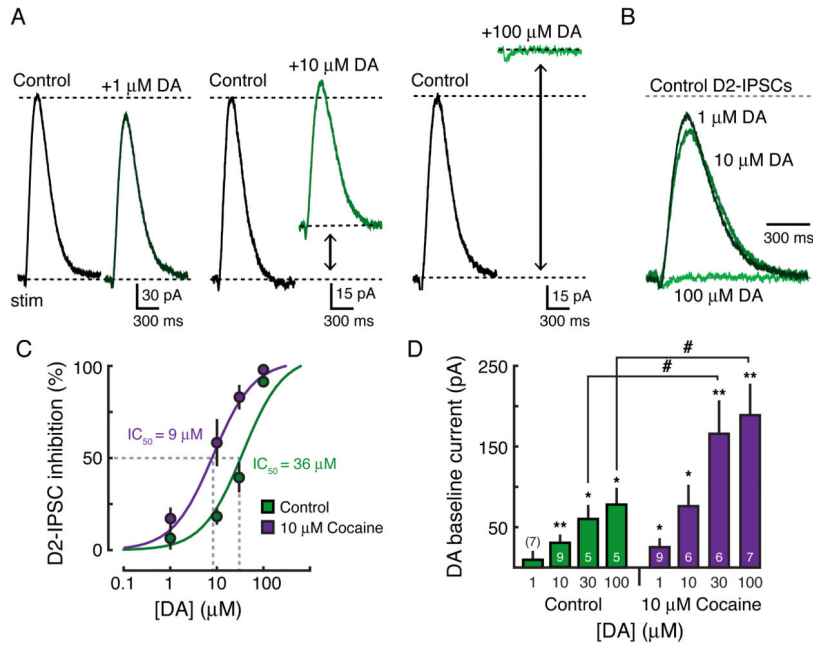


**Figure 4. High Dopamine Concentrations Saturate D2-receptors in MSNs**

(A) Representative whole-cell recordings in the presence of 1  $\mu\text{M}$  (left), 10  $\mu\text{M}$  (middle), and 100  $\mu\text{M}$  (right) dopamine. (B) Overlay of the dopamine traces shown in A illustrating that higher concentrations are necessary to significantly occlude the D2-IPSC. IPSCs have been normalized to control baseline levels. (C) Concentration-response curve under control conditions (green) and in the presence of 10  $\mu\text{M}$  cocaine (purple) showing the decrease in IPSC amplitude induced by bath application of dopamine (control:  $\text{IC}_{50} = 36 \mu\text{M}$ ; cocaine:  $\text{IC}_{50} = 9 \mu\text{M}$ ). (D) Summary data illustrating the increase in baseline outward current under control conditions (green) and in 10  $\mu\text{M}$  cocaine (purple) in the presence of different concentrations of exogenous dopamine (control:  $\text{EC}_{50} = 18 \mu\text{M}$ ; cocaine:  $\text{EC}_{50} = 16 \mu\text{M}$ ). Error bars indicate  $\pm$  SEM. \* =  $p < 0.05$  and \*\* =  $p < 0.01$  by one-sample Student's  $t$  test. # =  $p < 0.05$  by Student's unpaired  $t$  test. Numbers in bar graphs represent number of cells recorded.

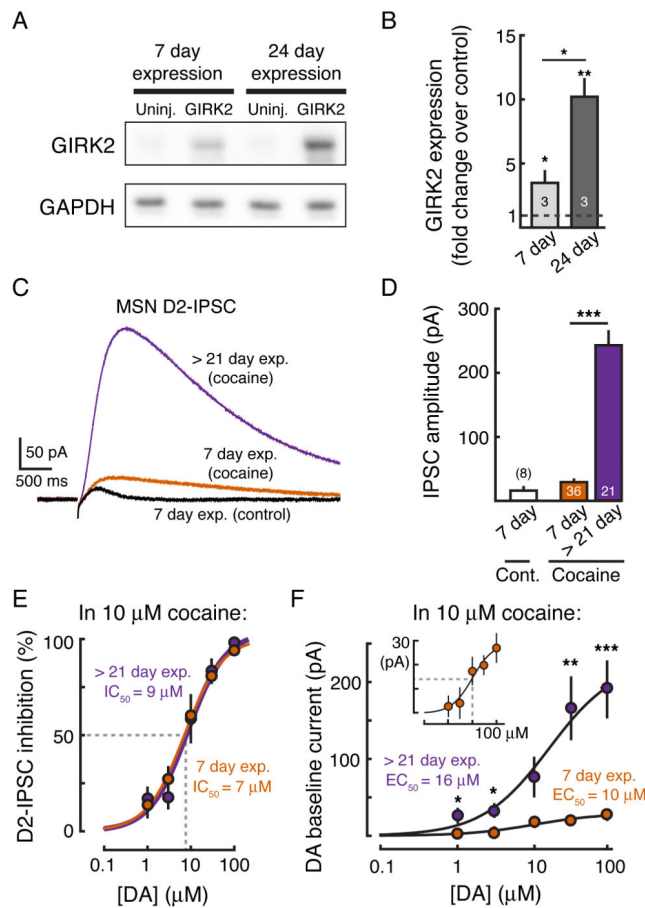


**Figure 5. GIRK Overexpression Does Not Affect the Affinity of D2-receptors**

(A) Representative western blot showing GIRK2 protein overexpression at 7 and 24 days following AAV injection. GAPDH is shown as a loading control. (B) Quantification showing the fold-increase in GIRK2 expression at 7 and 24 days following AAV injection. Expression levels of GIRK2 were normalized to GAPDH. Fold change was calculated with respect to GIRK2 levels in the respective uninjected hemisphere. Numbers in bar graph represent number of animal replicates. (C) D2-IPSC recorded from GIRK2<sup>+</sup> MSNs in brain slices from mice either 7 days (control–black, and in 10 μM cocaine–orange) (range: 5 to 9) or > 21 days (in 10 μM cocaine - purple) after AAV injection. (D) Summary data showing the amplitude of the D2-IPSC in mice with 7-day and > 21-day expression of GIRK2. The increase in IPSC amplitude from day 7 to day 21 following injection reflects the increase in GIRK2 expression. Numbers in bar graphs represent number of cells recorded. (E) Concentration-response curve for the inhibition of the D2-IPSC by bath application of dopamine (performed in 10 μM cocaine) in GIRK2 injected mice with > 21-day (purple) and 7-day (orange) expression. No change in the IC<sub>50</sub> is seen (> 21-day: IC<sub>50</sub> = 9 μM; 7-day: IC<sub>50</sub> = 7 μM). (F) Concentration-response curve for the outward current produced by bath application of dopamine (performed in 10 μM cocaine) in GIRK2 injected mice with > 21-day (purple) and 7-day (orange) expression. There is an increase in the maximum effect produced by 100 μM dopamine (> 21-day: 190 ± 36 pA, n = 7; 7-day expression: 27 ± 6 pA, n = 11), but there is no change in the EC<sub>50</sub> (24-day: EC<sub>50</sub> = 15 μM, n = 7; 7-day: EC<sub>50</sub> = 10

$\mu\text{M}$ ,  $n = 11$ ). Error bars indicate  $\pm$  SEM. \* =  $p < 0.05$ , \*\* =  $p < 0.01$ , \*\*\* =  $p < 0.001$  by Student's  $t$  test.

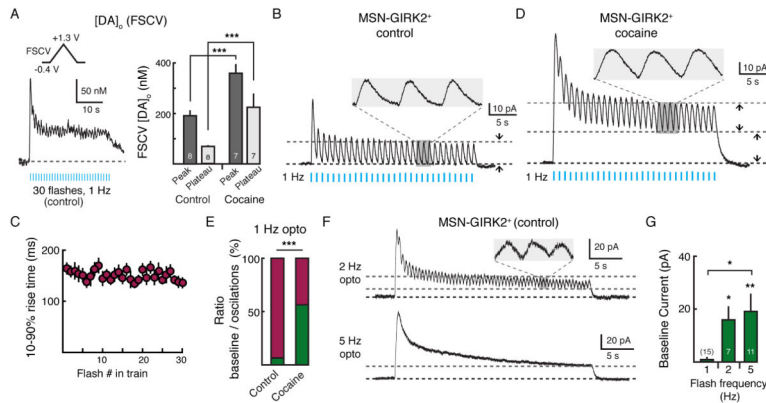


**Figure 6. Transporters Limit Sustained Activation of D2-receptors**

(A) FSCV measurements of the  $[DA]_o$  following repetitive optogenetic stimulation of striatal ChR2-expressing dopamine terminals. During 1 Hz optogenetic stimulation (30 seconds, 2 ms pulse) the  $[DA]_o$  peaked and then maintained a plateau for the duration of the train. Right: Summary of the  $[DA]_o$  evoked following 1 Hz (30 seconds, 2 ms pulse) stimulation under control conditions and in the presence of cocaine (3  $\mu$ M). Numbers by bar graphs represent number of slices used to measure  $[DA]_o$ . Light intensity was set so as to produce ~50% maximum amplitude D2-IPSCs (~0.4 mW) in a separate set of slices expressing both GIRK2 and ChR2. (B) Electrophysiological recording from a GIRK2<sup>+</sup> MSN following similar optogenetic stimulation of striatal dopamine terminals expressing ChR2 (1 Hz, 30 seconds, 2 ms pulse). At 1 Hz, stimulation evokes discrete oscillations in GIRK2<sup>+</sup> MSNs with no change in baseline holding current. Trace is the average across nine GIRK2<sup>+</sup> MSNs. Insert, expanded trace showing oscillations. Pulse width = 2 ms. (C) Summary 10 - 90% rise time of each IPSC in the train (n = 9, p = 0.1, Pearson's correlation). (D) In the presence of cocaine (3  $\mu$ M), similar optogenetic stimulation of ChR2-expressing dopamine terminals induces an increase in the standing outward current in GIRK2<sup>+</sup> MSNs with superimposed phasic oscillations. Trace is the average across seven GIRK2<sup>+</sup> MSNs. (E) Summary data showing quantification of the oscillations (magenta) and shift in the apparent baseline (green) as components of the total outward current measured under control conditions (n = 15) and in 3  $\mu$ M cocaine (n = 13), as illustrated in B and D. A significant tonic component of the current is only seen when reuptake is blocked with cocaine (p < 0.001). (F) Increasing the frequency of optogenetic stimulation decreases the ratio of the phasic D2-IPSC to tonic standing outward current during the duration of the flash train. Top: 2 Hz stimulation; bottom: 5 Hz stimulation. (G) Summary of the amplitude of the baseline current resulting from different frequencies of optogenetic stimulation. Numbers in bar graphs represent number of cells recorded. Error bars indicate  $\pm$  SEM. \* = p < 0.05, \*\* = p < 0.01, \*\*\* = p < 0.001 by Student's t test.

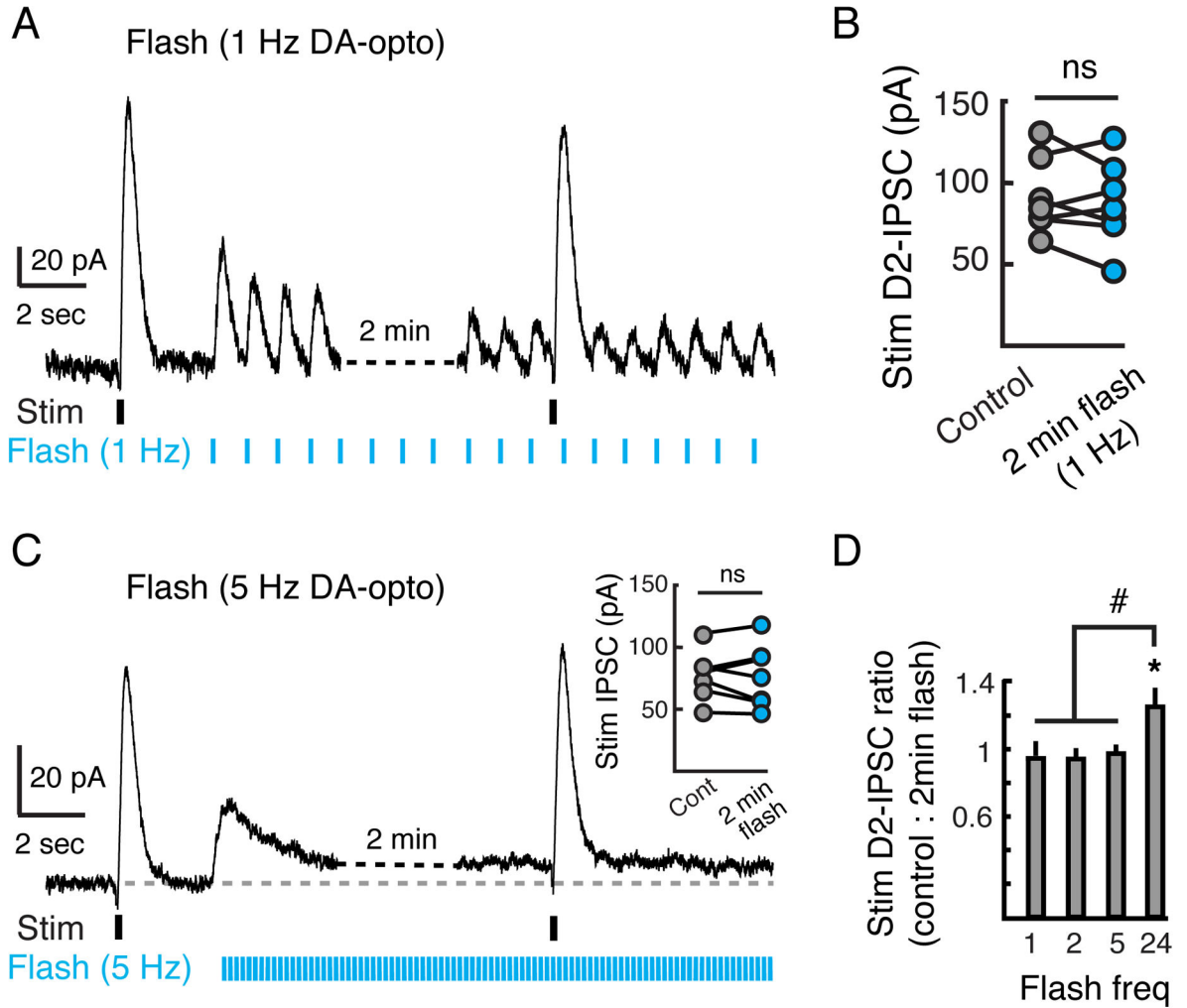


**Figure 7. D2-receptors on MSNs Respond to Both Tonic and Phasic Dopamine Release**  
**(A)** To mimic tonic firing of dopamine neurons in striatal slices, repetitive optogenetic stimulation (Flash) (2 min, 1 Hz, 2 ms pulse width, light intensity set to evoke D2-IPSC ~50% maximum amplitude, ~0.4 mW) was used while recording from GIRK2<sup>+</sup> MSNs. Electrical stimulation (Stim) (~95% maximum amplitude) was used to evoke a control D2-IPSC and a second D2-IPSC two minutes later during the sustained train of optogenetic stimulation. **(B)** Summary of the amplitude of electrically evoked control D2-IPSCs and IPSCs following 2 minutes of 1 Hz optogenetic stimulation. Each circle represents an individual cell (n = 7). There was no difference in the amplitude of D2-IPSCs pre- and post-optogenetic stimulation. **(C)** Repeated experiment as in **A** but using 5 Hz optogenetic stimulation (n = 7). Inset: Summary of the amplitude of electrically evoked IPSCs. **(D)** Summary of the ratio of D2-IPSCs evoked by electrical stimulation before and after 2 minutes of optogenetic stimulation of dopamine terminals at 1, 2, 5 and 24 Hz. Only 24 Hz optogenetic stimulation facilitated the amplitude of D2-IPSCs. Error bars indicate  $\pm$  SEM.

ns =  $p > 0.05$  \* =  $p = 0.05$  by Student's paired  $t$  test. # =  $p < 0.05$  by one-way ANOVA, Tukey-Kramer test.